

# The Calcium Carbonate Geological Samples Study by $^3\text{He}$ NMR

Egor Alakshin<sup>1</sup> · Rasul Gazizulin<sup>2</sup> · Alex Klochkov<sup>1</sup> ·  
Ekaterina Kondratyeva<sup>1</sup> · Artem Laskin<sup>1</sup> ·  
Murat Tagirov<sup>1,3</sup>

Received: 1 April 2017 / Revised: 22 May 2017 / Published online: 1 June 2017  
© Springer-Verlag Wien 2017

**Abstract** Geological samples of calcium carbonates ( $\text{CaCO}_3$ ) were investigated by  $^3\text{He}$  NMR, nitrogen porosimetry, X-ray diffraction and electron microscopy methods. The integral porosity of the samples was obtained by  $^3\text{He}$  nuclear magnetic resonance method and compared with nitrogen adsorption isotherms data. The advantages of  $^3\text{He}$  porometry method are discussed.

## 1 Introduction

The main raw hydrocarbon resources become limited nowadays, which promotes development of difficult grounds and fields. A half of the World's hydrocarbon reserves are concentrated in carbonate oil reservoirs. A lot of them are likely to have a production lifetime beyond 50 years [1]. Usually carbonate reservoirs have fairly complicated structure and it is difficult to predict their output and recovery factor. Heterogeneous nature of porosity is one of the most important topical problems [1, 2].

Terrigenous collectors are characterized by the intraparticle type of porosity. The carbonate reservoir model basically can be represented as a cluster of blocks separated by micro- and macro-cracks and cavities. These cavities are the channels where the fluid movement occurs in the pore space. The pore space structure is one of the most important parameters for comprehensive evaluation of the collectors.

---

✉ Ekaterina Kondratyeva  
katarina.kondratyeva@gmail.com

<sup>1</sup> Institute of Physics, Kazan Federal University, Kremlevskaya 18, Kazan, Russian Federation 420008

<sup>2</sup> CNRS Institut Néel et Université Grenoble Alpes, B.P. 166, 38042 Grenoble, France

<sup>3</sup> Institute of Perspective Research, Academy of Sciences of the Republic of Tatarstan, L. Bulachnaya 36a, Kazan, Russian Federation 420111

Nowadays, a lot of methods for hollow sample space volume and pore size distribution estimation exist.

Porosimetry is an analytical technique used to determine a total pore volume, pore size distribution and surface area [3–7]. The typically used methods are mercury intrusion porosimetry (MIP), cryoporometry and nitrogen adsorption method. Mercury porosimetry provides detailed information on the pore volume and pore size distribution. But MIP method is sensitive to large capillary pores. However, mercury porosimetry is a destructive method of analysis due to high pressure applied to the sample during the measurement which can deform and destruct the sample [8].

The nuclear magnetic resonance (NMR) cryoporometry is widely used to determine pore sizes in porous materials. The NMR cryoporometry method is indirect method which determines the relative ratio of the amounts of substance in liquid and frozen state at different temperatures, since the melting temperature depends on the size of pores. The NMR method is capable to distinguish liquid and frozen state since there are substantial differences between the nuclear spin relaxation times in the two phases [9–15].

One of the most commonly used methods for determining the pore size distribution is the gas adsorption method. The main advantages of this method are the simplicity of the measurements and the ability to determine the specific surface area and pore size distribution, the volume of micro- and meso-pores and the total pore volume. The gas adsorption method is used to analyze pores in the range from 0.35 to 100 nm [16]. By analysis of adsorption and desorption isotherms using the Barrett–Joyner–Halenda (BJH) and Brunauer–Emmett–Teller (BET) methods, it is possible to determine the surface area of the adsorbent, the pore size distribution and the total pore volume. The BET method can be used to determine the surface area of the adsorbent with an accuracy of 5–10% in the range  $P/P_0 = 0.05–0.35$ , where  $P/P_0$  is the ratio of the partial pressure of the adsorbed substance to the saturated vapor pressure of the adsorbed gas. For a more detailed analysis of the porous structure such as a pore volume and pore size distribution, the BJH method is used. The BJH method can be applied in the range of relative pressures  $P/P_0 = 0.4–0.967$  [17, 18].

The  $^3\text{He}$  NMR is used to study various porous substrates [19–25]. Recently [20, 21], this method has been proposed for characterization of clay geological samples.

In the present article, the calcium carbonate geological samples were characterized using scanning electron microscopy (SEM), X-ray diffraction (XRD), NMR of liquid  $^3\text{He}$  and nitrogen porosimetry.

## 2 Samples

Core cuts from the South-Eastern part of the Republic of Tatarstan (Russia) were used as samples. These samples are dated to carbonate deposits of Verey-Bashkir age period. They are composed of interbedded limestones and dolomites with different porosity with clay layers inclusions.

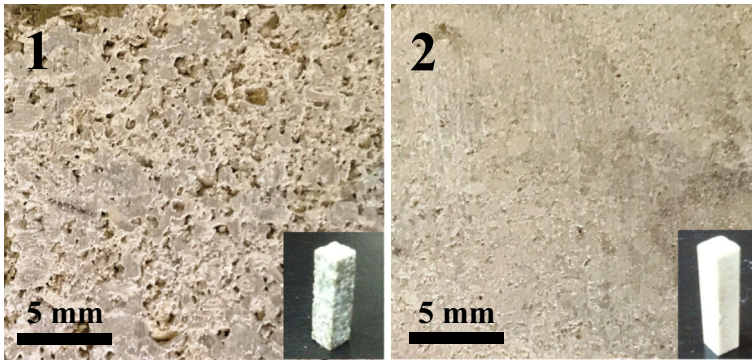


**Fig. 1** Images of calcium carbonate geological samples #1 and #2

The samples were cut out in the shape of a parallelepiped with  $13.5 \times 3.5 \times 3.5 \text{ mm}^3$  size. The photographic images of the samples are shown in Fig. 1.

### 3 Characterization

The geological samples were studied using SEM and XRD techniques. SEM images (Fig. 2) were obtained by Carl Zeiss: Merlin emission scanning electron microscope (accelerating voltage 5 kV, probe current 300 pA).

XRD measurements were performed using Bruker D8 Advance X-ray diffractometer with copper  $K\alpha$  ( $\lambda = 1.5418 \text{ \AA}$ ) radiation using continuous scan. Scan speed was set to  $0.005^\circ/\text{s}$  in the range of diffraction angles  $20^\circ\text{--}60^\circ$ . Experimental XRD patterns of calcium carbonate geological samples #1 and sample #2 are presented in Fig. 3.

The XRD patterns confirm the crystalline structure of the geological samples and they are in a good agreement with standard patterns of  $\text{CaCO}_3$  carbonates. It can be seen that intensity of additional peaks of XRD pattern is negligibly low, so there are no significant presence of other crystal phases in these samples.

### 4 Nitrogen Porosimetry

The nitrogen adsorption and desorption isotherms were measured by Autosorb-iQ equipment at 77 K. Figure 4 shows the nitrogen adsorption and desorption isotherms measured for sample #1 and sample #2.

The porosity of the samples was determined from BJH method adsorption by the following equation:

$$\text{Porosity} = \frac{V_T}{V_s} \times 100\%, \quad (1)$$

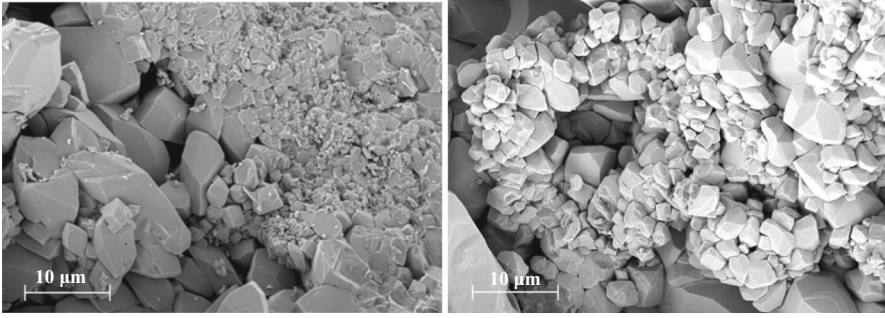


**Fig. 2** SEM images of calcium carbonate geological samples #1 (left) and #2 (right)

**Fig. 3** XRD patterns of sample #1 (a) and sample #2 (b) and the standard data of  $\text{CaCO}_3$  (c)

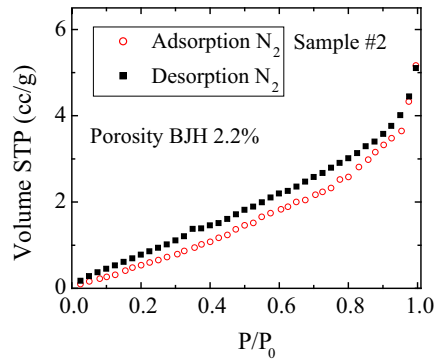
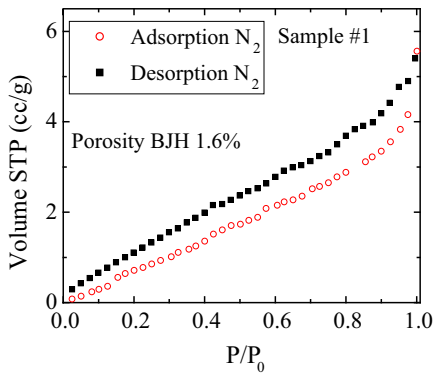
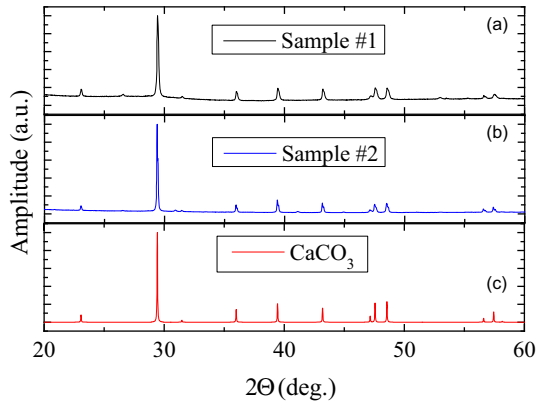


**Fig. 4** Adsorption and desorption isotherms measured for sample #1 (left) and sample #2 (right)

where  $V_T$  is the total pores volume of the sample (the maximum amount of adsorbed gas at  $\frac{P}{P_0} = 0.99$ ),  $V_s$  is the volume of sample. Obtained porosity by BJH method is about 1.6% for sample #1 and 2.2% for sample #2.

## 5 The $^3\text{He}$ NMR Porometry

The  $^3\text{He}$  atoms are able to penetrate into smaller pores and cracks that are inaccessible for larger gas molecules such as nitrogen  $\text{N}_2$  and hydrogen  $\text{H}_2$ , because of inert nature and smaller molecular size of  $^3\text{He}$  (the kinetic diameter of  $^3\text{He}$  is 0.26 nm compared to 0.36 nm for  $\text{N}_2$  molecule [26]). In this section, the advantages of  $^3\text{He}$  NMR porometry will be outlined.

The home-built pulse NMR spectrometer (frequency range of 3–25 MHz) with a resistive magnet (up to 0.8 T) was used for NMR experiments [27]. Temperature 1.5 K was achieved by liquid helium vapor pumping. The  $^3\text{He}$  NMR Larmor frequency was 11.16 MHz at 344 mT external magnetic field. The sample was placed in a Pyrex cell (outer diameter of 6 mm), which was leak-tight connected to a  $^3\text{He}$  gas handling system. The sample was pumped out to a pressure of  $10^{-3}$  Torr before NMR experiments. The NMR coil was mounted on the surface of glass cell. The design of experimental cell is shown in Fig. 5. During experiments, liquid  $^3\text{He}$  was condensed into the sample cell at 1.5-K temperature and filled the pores of the samples and the residual volume of the cell. The liquid  $^3\text{He}$  outside of the sample was used as a reference to estimate the integral porosity. The NMR parameters of liquid  $^3\text{He}$  in the pores and outside of the sample (calibration cavity) significantly differ [20].

The “saturation–recovery” sequence was used for the measurement of  $^3\text{He}$  spin–lattice relaxation time  $T_1$ . Figure 6 shows the experimental curves of the nuclear longitudinal magnetization recovery of liquid  $^3\text{He}$  in contact with samples #1 and #2.

Solid lines represent approximation using Eq. (2) with presented parameters.

The longitudinal magnetization recovery curves (Fig. 6) can be described with the following equation based on the model of experiment:

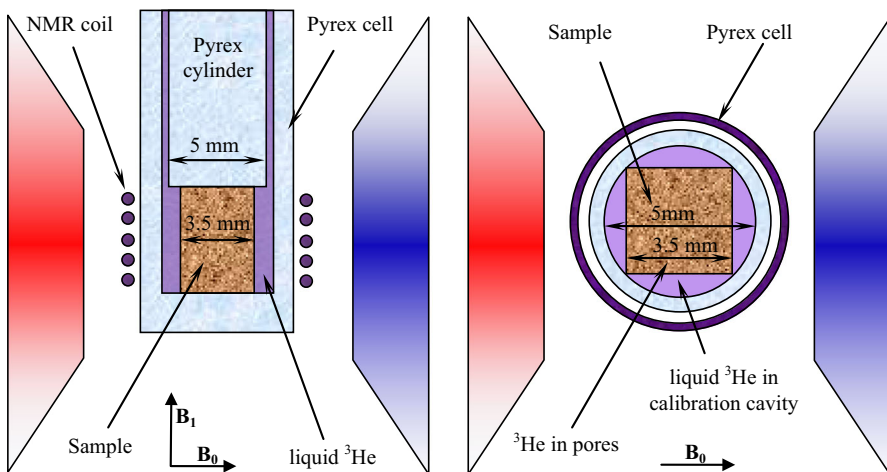


**Fig. 5** Design of NMR experiments: side view (left), top view (right)

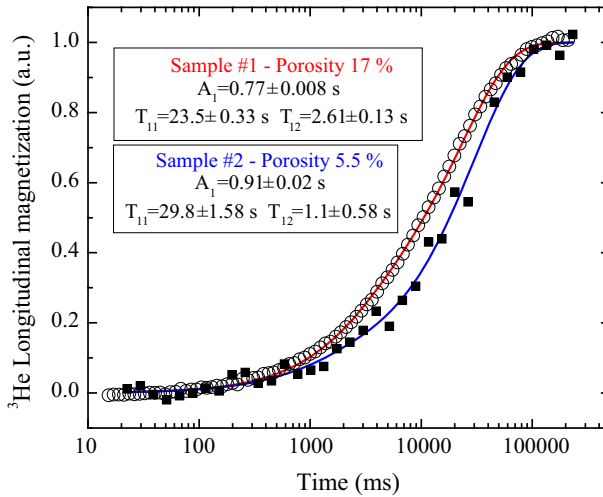


**Fig. 6** Longitudinal magnetization recovery curves of liquid  $^3\text{He}$  nuclei in contact with the samples #1 and #2

$$A = 1 - A_1 \exp\left(-\frac{\tau}{T_{11}}\right) - (1 - A_1) \exp\left(-\frac{\tau}{T_{12}}\right), \quad (2)$$

where  $A_1$  is the relative fraction of  $^3\text{He}$  in the calibration cavity,  $T_{11}$  is the spin–lattice relaxation time of  $^3\text{He}$  in the calibration cavity,  $T_{12}$  is the spin–lattice relaxation time of  $^3\text{He}$  in pores of calcium carbonate sample. The following value was obtained from the fit for the sample #1:  $A_1 \approx 0.77$ . Based on the geometrical dimensions of the sample and the calibration cavities, it is possible to estimate porosity of the sample, which in the case of sample #1 is about 17%. The obtained porosity of the sample #2 is about 5.5% ( $A_1 \approx 0.91$ ).

The porosity values obtained by the  $^3\text{He}$  NMR method significantly exceed the values obtained by nitrogen porosimetry and correlated with images on Fig. 1. Most likely, this is due to the fact that  $^3\text{He}$  atoms can penetrate into smaller pores and cracks (bigger than the kinetic diameter of  $^3\text{He}$ ), because of inert nature and smaller molecular size of  $^3\text{He}$  in contrast to nitrogen molecules  $\text{N}_2$ , as well as  $^3\text{He}$  fills up micro-pores, invisible for nitrogen porosimetry. It need to be mentioned that  $^3\text{He}$  can sneak into smallest pores among other gases, but void volume of crystal structure remains intact. It is known that the range of visible pores for nitrogen porosimetry is about 0.35–100 nm [16].

The  $^3\text{He}$  NMR method is sensitive to all pores with a diameter larger than 0.26 nm and the range is much wider, compared to nitrogen porosimetry, which is a significant advantage of the  $^3\text{He}$  NMR method of porometry.

## 6 Conclusions

Various methods exist for studying geological samples, but some of the traditional methods are not suitable for some substrates or provide unreliable data. For instance, the integral porosity measurements for substrates with low porosity or so-called closed porous substrates demand new methods to be implemented. The  $^3\text{He}$  NMR at low temperatures is a suitable technique for such application. In this article, the NMR data of  $^3\text{He}$  in pores of carbonates are reported and the value of integral porosity was estimated. The obtained results prove that  $^3\text{He}$  NMR technique has advantages over nitrogen adsorption methods because it allows to detect pores in wider range.

**Acknowledgements** We are grateful to Safiullin K.R., Kuzmin V.V., Solomonov B.N. and Kosarev V.E. for fruitful discussions. The work is performed according to the Russian Government Program of Competitive Growth of Kazan Federal University.

## References

1. T.P. Burchette, *Geol. Soc. Special Publ.* **370**, 17 (2012)
2. C. Genty, J.L. Jensen, W.M. Ahr, *Nat. Resour. Res.* **16**, 45 (2007)
3. L.M. Anovitz, D.R. Cole, *Rev. Mineral. Geochem.* **80**, 61 (2015)
4. A.T. Watson, C.T.P. Chang, *Prog. Nucl. Magn. Reson. Spectrosc.* **31**, 343 (1997)
5. B. Vincent, M. Fleury, Y. Santerre, B. Brigaud, *J. Appl. Geophys.* **74**, 38 (2011)
6. Z. Hossain, C.A. Grattoni, M. Solymar, I.L. Fabricius, *Pet. Geosci.* **17**, 111 (2011)
7. S. Anferova, V. Anferov, D.G. Rata, B. Blumich, J. Arnold, C. Clauser, P. Blumer, H. Raich, *Concepts Magn. Reson. Part B Magn. Reson. Eng.* **23**, 26 (2004)
8. A.B. Abell, K.L. Willis, D.A. Lange, *J. Colloid Interface Sci.* **211**, 39 (1999)
9. J. Mitchell, J.B.W. Webber, J.H. Strange, *Phys. Rep.* **461**, 1 (2008)
10. Z.-P. Wang, C.-M. Huang, T. Wang, *J. Build. Mater.* **15**, 6 (2012)
11. J.H. Strange, M. Rahman, E.G. Smith, *Phys. Rev. Lett.* **71**, 3589 (1993)
12. E.W. Hansen, R. Smidh, M.J. Stocker, *J. Phys. Chem.* **100**, 11396 (1996)
13. P.A.C. Gane, C.J. Ridgway, E. Lehtinen, R. Valiullin, I. Furo, J. Schoelkopf, H. Paulapuro, J. Daicic, *Ind. Eng. Chem. Res.* **43**, 7920 (2004)
14. J. Warnock, D.D. Awschalom, M.W. Shafer, *Phys. Rev. Lett.* **57**, 1753 (1986)
15. O.V. Petrov, I. Furo, *Prog. Nuclear Magn. Reson. Spectrosc.* **54**, 97 (2009)
16. A.G. Khokhlov, R.R. Valiullin, J. Kärger, M.A. Stepovich, *Colloid J.* **70**, 507 (2008)
17. E.P. Barrett, L.G. Joyner, P.P. Halenda, *J. Am. Chem. Soc.* **73**, 373 (1951)
18. S. Brunauer, P.H. Emmett, E. Teller, *J. Am. Chem. Soc.* **60**, 309 (1938)
19. M.S. Tagirov, A.N. Yudin, G.V. Mamin, A.A. Rodionov, D.A. Tayurskii, A.V. Klochkov, R.L. Belford, P.J. Ceroke, B.M. Odintsov, *J. Low Temp. Phys.* **148**, 815 (2007)
20. R.R. Gazizulin, A.V. Klochkov, V.V. Kuzmin, K.R. Safiullin, M.S. Tagirov, A.N. Yudin, V.G. Izotov, L.M. Sitdikova, *Appl. Magn. Reson.* **38**, 271 (2010)
21. R.R. Gazizulin, A.V. Klochkov, V.V. Kuzmin, K.R. Safiullin, M.S. Tagirov, A.N. Yudin, *Magn. Reson. Solids* **11**, 33 (2009)
22. E.M. Alakshin, R.R. Gazizulin, A.V. Klochkov, V.V. Kuzmin, M.S. Tagirov, D.A. Tayurskii, N. Mulders, *J. Phys. Conf. Ser.* **324**, 012028 (2011)
23. A.V. Klochkov, M.S. Tagirov, *Low Temp. Phys.* **41**, 50 (2014)
24. E.M. Alakshin, R.R. Gazizulin, M.Y. Zakharov, A.V. Klochkov, E.V. Morozov, T.M. Salikhov, T.R. Safin, K.R. Safiullin, M.S. Tagirov, O.B. Shabanova, *Low Temp. Phys.* **41**, 39 (2015)
25. E.M. Alakshin, M.Y. Zakharov, A.V. Klochkov, V.V. Kuzmin, K.R. Safiullin, A.A. Stanislavovas, M.S. Tagirov, *JETP Lett.* **104**, 315 (2016)
26. J. Vermesse, D. Vidal, P. Malbrunot, *Langmuir* **12**, 4190 (1996)
27. E.M. Alakshin, R.R. Gazizulin, A.V. Klochkov, V.V. Kuzmin, A.M. Sabitova, T.R. Safin, M.S. Tagirov, *Magn. Reson. Solids* **15**, 13104 (2013)